

## **ANALYSIS OF ELECTROMAGNETICS SCATTERING FROM REFLECTOR AND CYLINDRICAL ANTENNAS USING WAVELET-BASED MOMENT METHOD**

**M. Lashab**

Département d'Électronique  
Université du 20 Août 55  
Skikda, Algeria

**F. Benabdelaziz and C. Zebiri**

Département d'Électronique  
Université de Mentouri  
Constantine, Algeria

**Abstract**—The aim of this work is to introduce the application of wavelet in Electromagnetic Scattering and making improvement in the moment method development. The conventional moment method basis and testing functions are used to digitalize the integral equations of the electric or magnetic field, resulting in dense matrix impedance. By using the wavelet expansion, wavelets as basis and testing functions, a sparse matrix is generated from the previous moment method dense matrix, which may save computational cost. Here application has been made upon two types of two dimensional antennas, which are circular cylindrical antennas and parabolic reflector antennas. Results are compared to the previous work done and published, excellent results are obtained.

### **1. INTRODUCTION**

The paper presents an analysis of two dimensional structures antennas using Wavelet-Based Moment Method and special application here is given to parabolic reflector antennas, and circular cylindrical antennas. Classical methods such as the Geometrical Theory of Diffraction (GTD), and Physical Optics (PO), cannot give accurate result especially for more complicated Geometries. Moment method is an accurate numerical method, the density of current upon the surface

of the antennas is modelled as a set of functions, the Electric Field Integral Equation (EFIE) is digitalized and the matrix system has to be solved. Moment Method needs huge computational time and space memory, for this reason it cannot be applied to antennas larger than a few wavelengths. By using the wavelets expansions, the basis and testing functions are chosen as orthogonal wavelets type, so that to enable sparse the impedance matrix, which lead to reducing memory space and computationally cost.

Although several fast algorithms have been used to reduce the computational complexity and memory requirement, such as Finite Element Method (FEM) [5], which formulate the electromagnetic problem using differential equation, And more power method such as the Fast Multi-pole Method or the Multilevel Fast Multi-pole Algorithm (MLFMA) [9], which need more powerful machine to be implemented. In contrast, Wavelet-Based Moment method which can be implemented easily in personal computer.

At first the paper treats circular cylinder antennas with perfect conducting type, the radar cross section (RCS) and the density of current are presented and compared with available published work [7, 10, 3]. Secondly dealing with the parabolic reflector, which is considered also to be electrically perfect conductor (PEC) and feed by a finite dipole. The radar cross section (RCS) and the radiation patterns for the parabolic reflector are analyzed, illustrated and compared to theoretical and published work [8].

## 2. FORMULATION

### 2.1. Integral Equation

On a two dimensional contour antennas, and for Perfect Electric Conducting Surface, the boundary conditions on the surface are expressed as:

$$\hat{n} \times \vec{E} = \hat{n} \times (\vec{E}_i + \vec{E}_s) = 0 \quad (1)$$

and

$$\hat{n} \times \vec{H} = \hat{n} \times (\vec{H}_i + \vec{H}_s) = J_s \quad (2)$$

where  $\hat{n}$ , is the unit vector normal to the surface and  $J_s$  the current density, for the reflector antennas the incident field is from the illumination feed considered as dipole which is:

$$E^i(\theta_i, r_i) = G_{feed}(\theta_i, r_i) \frac{e^{-j.k.r_i}}{r_i} \quad (3)$$

where  $G_{feed}$  is the feed function, for 2D problem the field is on the  $Z$  axis, equation (3) can be approximated for ( $kr \gg 1$ ), to:

$$G_{feed}(\theta_i, r_i) = \sin(\theta_i) \hat{\theta}$$

where:

$$r_i = x \cdot \cos(\theta_i) + y \cdot \sin(\theta_i)$$

For the cylindrical antennas the incident field for TM polarization is given by:

$$E_Z^i = e^{jk(x \cdot \cos(\phi_i) + y \cdot \sin(\phi_i))} \quad (4)$$

Using the boundary condition (1), the scattered field may be written as an integral of the induced current and the 2D Green's function, applying the Electric Field Integral Equation (EFIE) [6], this leads to Equation (5).

$$\frac{k\eta}{4} \int_C J_Z(r) H_0^2(k|r - r'|) dc' = E_Z^i(r) \quad (5)$$

where  $C$  is the contour of the cylindrical or reflector antennas, and  $H_0^{(2)}(k|r - r'|)$  is Hankel function of the second kind zero order. ( $J_z$  and  $E_z$  are in the  $z$  axis). Also using the boundary condition (2), and applying the Magnetic Field Integral Equation (MFIE) [6], as:

$$\begin{aligned} -H_i(r) &= \frac{J_c(r)}{2} + \\ &+ j\frac{k}{4} \int_C J_c(r') \cdot H_1^{(2)}(k|r - r'|) \cdot \cos(\psi_{r,r'}) \cdot dc' \end{aligned} \quad (6)$$

where  $H_1^{(2)}(k|r - r'|)$  is the Hankel function of the second kind first order,  $\psi_{r,r'}$  is the angle between the normal vector ( $\hat{n}$ ), and ( $r - r'$ ) vector. The reflector antennas fed by the dipole antenna, studied here is presented in Figure 1, and the circular cylinder antenna in Figure 2.

Equation (5) can be expressed for two dimensional antennas, and for the (PEC) circular cylinder type as:

$$\frac{k\eta}{4} \int_{\theta=0}^{\theta=2\pi} J_z(r) \cdot H_0^{(2)}(kR) \cdot |r'(\theta)| \cdot d\theta = E_z^i(r) \quad (7)$$

where:  $R = |r - r'| = \sqrt{(x - x')^2 + (y - y')^2}$ .

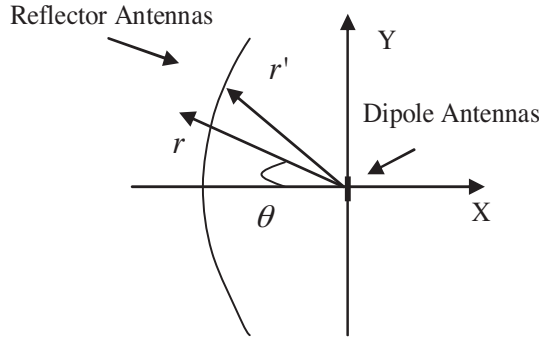


**Figure 1.** Reflector antennas feed by dipole antennas.

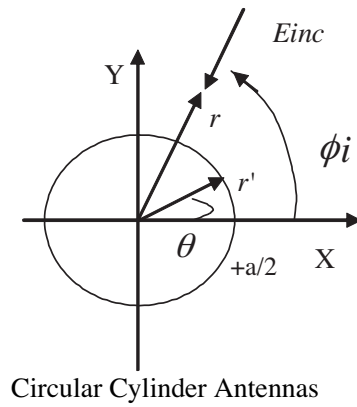


**Figure 2.** PEC cylindrical antennas polarized by incident wave.

In the same manner Equation (6) can be expressed for two dimensional antennas as:

$$-H_z^{inc}(\theta) = J(\theta) \frac{\delta_{r,r'}}{2} + j \frac{k}{4} \int_{\theta=0}^{\theta=2\pi} J(\theta') H_1^{(2)}(k|r-r'|) \cdot \cos(\psi_{r,r'}) |r'(\theta')| .d\theta' \quad (8)$$

where  $\delta_{r,r'}$  is the Kronecker delta function defined by

$$\delta_{r,r'} = \begin{cases} 1 & r = r' \\ 0 & r \neq r' \end{cases}$$

## 2.2. Moment Method Formulation

The induced current can be found when using the Moment Method [2], and expand this current in a series of  $N$  basis functions, given by:

$$J_z = \sum_n I_n \cdot F_n \quad (9)$$

where the  $F_n$  are the basis functions and the  $I_n$  are the unknown constants, and using  $M$  similar testing functions ( $g_m$ ), the inner product for the TM mode can be written as

$$\sum_{n=1}^N \left\langle g_m, \frac{\omega\mu_0}{4} \int_{\theta=0}^{\theta=2\pi} F_n \cdot H_0^{(2)}(R) \cdot |r'(\theta)| \cdot d\theta \right\rangle I_n = \langle g_m, E_z^{inc}(r) \rangle, \quad (10)$$

for  $m = 1 \dots M$ .

Finally Equation (10) can be written as a matrix form:

$$[Z_{mn}] \cdot [I_n] = [U_m] \quad (11)$$

where  $[Z_{m,n}]$  is the impedance matrix, and  $[I_n]$  are the unknown constants and  $[U_m]$  is the voltage matrix .

$$[I_n] = [Z_{mn}]^{-1} \cdot [U_n] \quad (12)$$

## 2.3. Wavelet Expansions

The basis and testing functions are presented as a superposition of wavelets at several scales including the scaling function. A Galerkin method is then applied, where the set of basis functions used to present the current function, are used as weighting functions. The wavelets used here are Daubechies basis an orthogonal type, its study is useful from theoretical point of view, because it offers an intuitive understanding of many multi-resolution properties. Furthermore, due to its simplicity Daubechies wavelets are widely employed. The scaling function is  $\phi(x)$ , and the mother wavelet function is  $\psi(x)$  [6], the scaling and the mother wavelets functions are defined by:

$$\phi_{jn}(x) = 2^{j/2} \phi(2^j x - n) \quad (13)$$

$$\psi_{mn}(x) = 2^{m/2} \psi(2^m x - n) \quad (14)$$

where ( $m$  or  $j$ ) are the resolution level and ( $n$ ) is the translation factor. The wavelets are applied directly upon the integral equation. The

density of current will be represented as a linear combination of the set wavelets functions and scaling functions as follow:

$$Jz(x) = \sum_n a_n \cdot \phi_{j,n}(x) + \sum_{m=j}^{2^j-1} \sum_n c_{m,n} \psi_{m,n}(x) \quad (15)$$

The fact that the wavelets are orthogonal and the presence of vanishing moment, this is enabling sparse matrix production. When applying Equation (10) into (15) and for the TM case, we obtain the set of matrix equation as follow:

$$\begin{bmatrix} [Z_{\phi,\phi}] & [Z_{\phi,\psi}] \\ [Z_{\psi,\phi}] & [Z_{\psi,\psi}] \end{bmatrix} \begin{bmatrix} a_n \\ c_{m,n} \end{bmatrix} = \begin{bmatrix} \langle E_z^{inc}, \phi_{j,n} \rangle \\ \langle E_z^{inc}, \psi_{m,n} \rangle \end{bmatrix} \quad (16)$$

where:

$$[Z_{\phi,\phi}] = \left\langle \phi_{j,n}, \frac{\omega\mu_0}{4} \int_{\theta=0}^{\theta=2\pi} \phi_{j,n} \cdot H_0^{(2)}(R) \cdot |r'(\theta')| \cdot d\theta \right\rangle \quad (17)$$

$$[Z_{\phi,\psi}] = \left\langle \phi_{j,n}, \frac{\omega\mu_0}{4} \int_{\theta=0}^{\theta=2\pi} \psi_{m,n} \cdot H_0^{(2)}(R) \cdot |r'(\theta')| \cdot d\theta \right\rangle \quad (18)$$

$$[Z_{\psi,\phi}] = \left\langle \psi_{m,n}, \frac{\omega\mu_0}{4} \int_{\theta=0}^{\theta=2\pi} \phi_{j,n} \cdot H_0^{(2)}(R) \cdot |r'(\theta')| \cdot d\theta \right\rangle \quad (19)$$

$$[Z_{\psi,\psi}] = \left\langle \psi_{m,n}, \frac{\omega\mu_0}{4} \int_{\theta=0}^{\theta=2\pi} \psi_{m,n} \cdot H_0^{(2)}(R) \cdot |r'(\theta')| \cdot d\theta \right\rangle \quad (20)$$

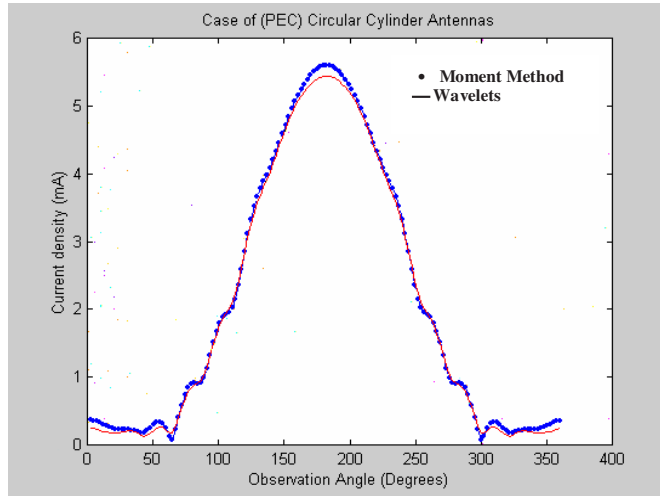
Since Galerkin Method employs the same testing functions and basis function, in the same manner is the equation for incident field is expressed. After then the unknown constants are determined, and the current density can be found using Equation (12), also the RCS which is directly related this latter, for TM case has been calculated.

### 3. NUMERICAL RESULTS

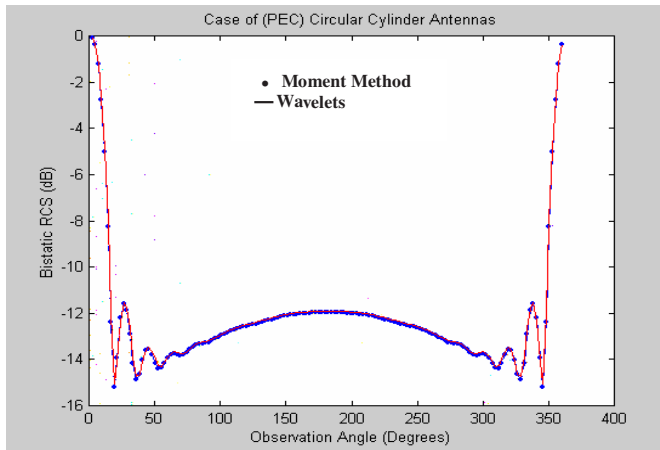
A computer program has been coded in Mat-lab language for the technique described above, the wavelet employed is constructed from Daubechies orthogonal wavelet with vanishing moment  $N = 7$ , the

lowest resolution level is chosen  $2^j = 2^7 = 128$ , since 128 wavelets are involved, a system of matrix (of  $128 \times 128$  elements) is generated.

The density of current for TM case has been given for circular cylinder of ( $1.5\lambda$  Diameter), and an incident Angle  $\phi_{inc} = 180^\circ$ , in



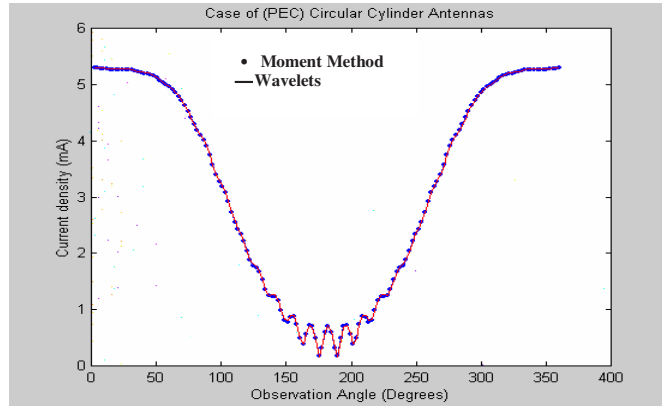
**Figure 3.** TM mode, density of current  $J_z$  for circular cylindrical antenna of diameter ( $a = 1.5\lambda$ ),  $\varphi_{inc} = 180^\circ$ .



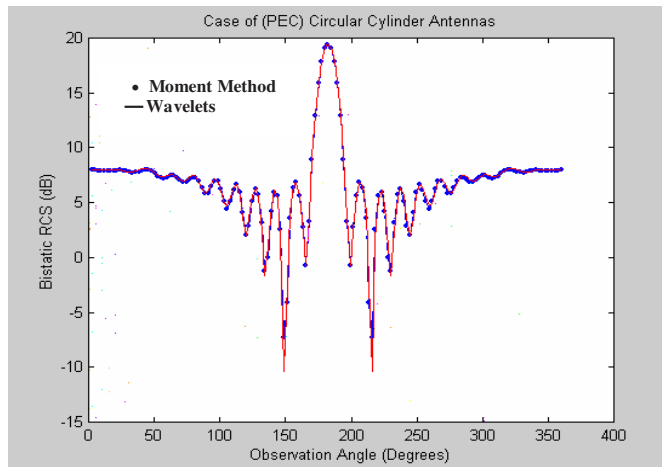
**Figure 4.** TM mode, bistatic RCS (dB) for circular cylindrical antenna of diameter ( $a = 1.5\lambda$ ),  $\varphi_{inc} = 180^\circ$ .

Figure 3, and for TE case circular cylinder has been studied, for ( $2\lambda$  Diameter) and incident Angle  $\phi_{inc} = 0^\circ$  in Figure 5. The Radar Cross Section (Bistatic RCS) for the two cases stated are presented in Figure 4 and Figure 6. Results are presented with comparison of traditional Moment Method and Wavelet-Based MoM. Results are Compared with previous work published [13] and [11].

The radiation pattern for H-plane and E-plane for the reflector



**Figure 5.** TE-mode, density of current  $J_\theta$  for (PEC) circular cylinder antennas of diameter ( $a = 2\lambda$ ),  $\varphi_{inc} = 0^\circ$ .



**Figure 6.** TE-mode, bistatic RCS (dB) for (PEC) circular cylindrical antenna of diameter ( $a = 2\lambda$ ),  $\varphi_{inc} = 0^\circ$ .



antenna feed by dipole has been presented for two cases first for  $F/D = 0.375$ , and  $D = 5\lambda$  in Figure 7 and Figure 8, and second with  $F/D = 0.96$ , and  $D = 10\lambda$  in Figure 9 and Figure 10. The two the cases presented with the two different methods the results show good agreement, for the classical moment method and for the wavelet-based

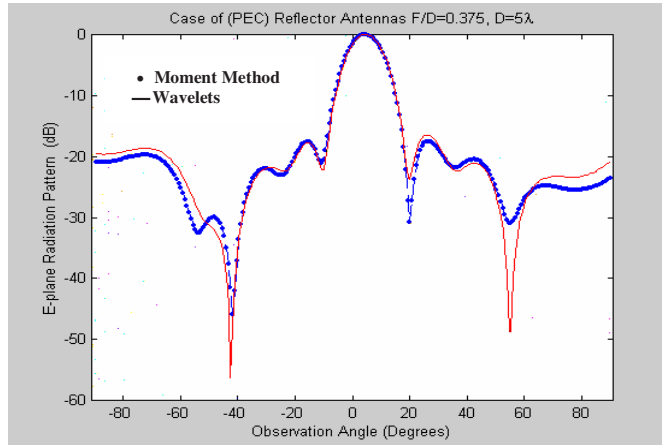


**Figure 7.** E-plane radiation pattern for parabolic reflector feed by dipole with  $F/D = 0.375$ , diameter of the reflector  $D = 5\lambda$ .

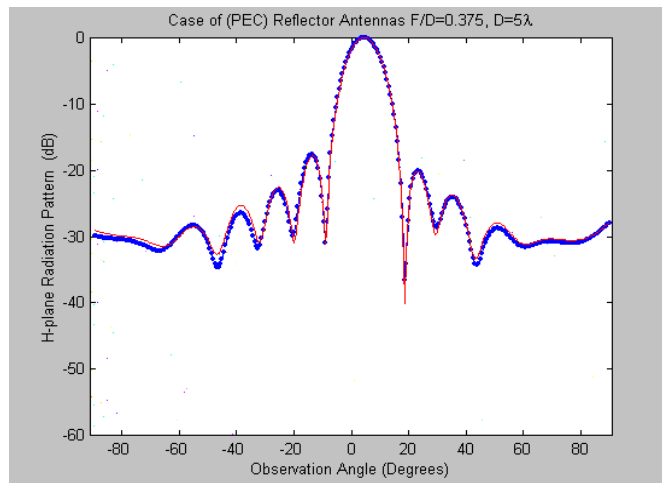


**Figure 8.** H-plane radiation pattern for parabolic reflector feed by dipole, with  $F/D = 0.96$ , diameter of the reflector  $D = 10\lambda$ .

moment method.

In this paper the use of Daubechies wavelet leads to a matrix sparsity of 78%, for a threshold of 3%, which means the moment matrices were rendered sparse by thresholding to zero all matrix

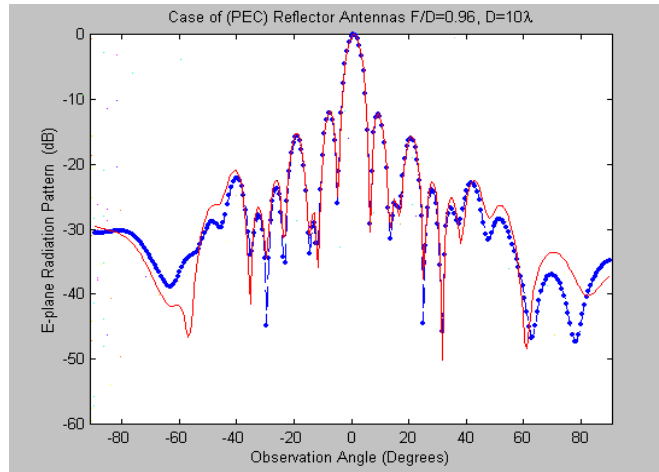


**Figure 9.** E-plane radiation pattern for parabolic reflector feed by dipole with  $F/D = 0.375$ , diameter of the reflector  $D = 5\lambda$ .

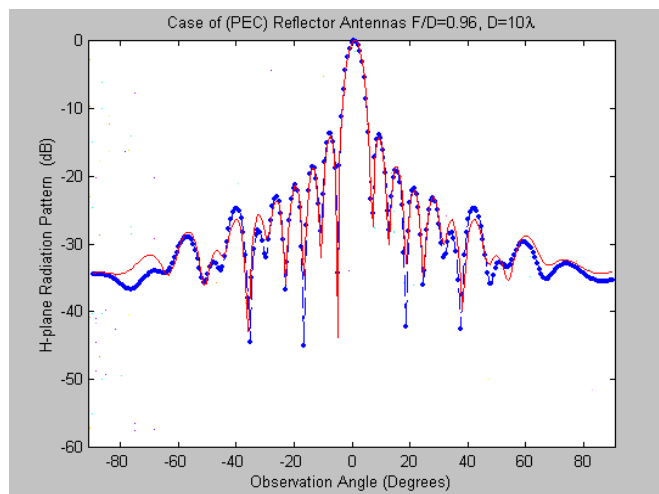


**Figure 10.** H-plane radiation pattern for parabolic reflector feed by dipole, with  $F/D = 0.96$ , diameter of the reflector  $D = 10\lambda$ .

elements whose magnitude was less than 3% of all the maximum magnitude of all matrix entries. However [12] has reached 85.5% with threshold of 2%, and using Haar wavelets.

It has been noticed that the time processing is inversely proportional to the threshold chosen for the sparsity of the matrix, which means that for low threshold the time processing is much longer.

#### 4. CONCLUSION

The analysis of electromagnetic scattering problem for two dimensional antennas using wavelets of Daubechies type has been presented for two types of antennas which are circular cylinder and reflector antennas feed by an infinitesimal dipole. The unknown current over the conducting surface has been expanded in terms of wavelets and scaling functions. After then a sparse matrix is generated, the resolution of the wavelet is set to  $2^7$  for threshold of 3% a sparsity of 78% is obtained, going for upper resolution enable accurate results but the impedance matrix became very heavy, so a compromise have to be made. The results obtained and compared to [1, 3, 8], they were successful.

#### REFERENCES

1. Capozzoli, A. and G. D'Elia, "Global optimization and antennas synthesis and diagnosis, Part two: Applications to advanced reflector antennas synthesis and diagnosis techniques," *Progress In Electromagnetics Research*, PIER 56, 233–261, 2006.
2. Balanis, C. A., *Antennas Theory Analysis and Design*, 2nd edition, John Wiley & Sons, Inc, New York, 1997.
3. Anastassiou, H. T., "Error estimation of auxiliary sources (MAS) for scattering from an impedance circular cylinder," *Progress In Electromagnetics Research*, PIER 52, 109–128, 2005.
4. Chou, H.-T., P. H. Pathak, Fellow IEEE, and R. J. Burkholder, "Novel Gaussian beam method for the rapid analysis of large reflector antennas," *IEEE Transactions and Antennas Propagation*, Vol. 49, No. 6, 880–891, June 2001.
5. Jin, J. M., *The Finite Element Methods in Electromagnetics*, John Wiley & Sons, New York, 1993.
6. Pan, G. W., *Wavelet in Electromagnetics and Devices Modelling*, John Wiley & Sons, Inc, New York, 2001.
7. Ye, Q., "Development of algorithms for solving electromagnetic interactions with large structures," *IEEE 1998 PhD Students Conference Gardcon'98 Proceeding Canada*, May 1998.

8. Ewe, W.-B., Student Member, L.-W. Li, Member, and Q. Wu, "Analysis of reflector and horn antennas using adaptive integral method," *IEICE Trans. Commun.*, Vol. E88-B, No. 6, 2327–2333, June 2005.
9. Zaw, Z. O. and E.-P. Li, "Analysis and design on aperture antenna systems with large electrical size using multilevel fast multipole method," *Journal of Electromagnetic Waves and Appl.*, Vol. 19, No. 11, 1485–1500, 2005.
10. Xiang, Z. and Y. Lu, "An effective hybrid method for electromagnetic scattering from inhomogeneous objects," *Progress In Electromagnetics Research*, PIER 17, 305–321, 1997.
11. Xiang, Z. and Y. Lu, "A hybrid FEM/BEM/WTM approach for fast scattering from cylindrical scatters with arbitrary cross section," *Progress In Electromagnetics Research*, PIER 22, 107–129, 1999.
12. Zunoubi, M. R. and A. A. Kishk, "A combined Bi-CGSTAB and wavelet transform method for em problems using moment method," *Progress In Electromagnetics Research*, PIER 52, 205–224, 2005.
13. Lashab, M., F. Benabdelaziz, and C. Zeberi, "On the use of wavelet-based moment method for analysis of two dimensional electromagnetic scattering, applied for circular and square contour antennas," *SETIT 2007*, 256, Tunisia, March 25–29, 2007.